2013 IEEE/RSJ International Conference on
Intelligent Robots and Systems (IROS)
November 3-7, 2013. Tokyo, Japan

Humanoid Self-correction of Posture Using a Mirror

Naohiro Hayashi, Tetsuo Tomizawa, Takashi Suehiro and Shunsuke Kudoh

***Abstract*— Humanoid robots have discrepancies between the postures simulated on models and those of actual humanoid bodies. To correct this problem, this paper proposes a method in which a robot observes its own posture in a mirror. This method does not need an additional time-consuming setup, such as calibration of external cameras. We attach a reference point to a known position on the robot body. By observing markers and the reference point in the same view, we can estimate the position of the markers accurately based on the geometric relationship between the mirror, an object, and its mirror reflection. We evaluate the proposed method by experiments of measuring and correcting the posture of an actual robot body to attain the target posture.**

***Index Terms*— Humanoid robot, mirror, Posture correction.**

I. INTRODUCTION

It is common practice to use a simulator to design the motion of a humanoid robot and then import the design into the robot. Discrepancies appearing between the postures of the simulated model and the actual robot lead to serious problems in controlling the robot. In practice, we observe differences caused by backlash, transmission errors in the gears, and warping of the body due to gravity (Fig. 1). A method for reducing such discrepancies is important in order to accurately control humanoid robots.

This paper proposes a method in which a robot stands in front of a mirror, observes itself, and corrects its own posture. As described in detail below, a geometric relationship exists between the mirror, the camera, the points on the robot, and the mirror images of these points, and we can use the relationship to improve the accuracy of the posture measurements. Our method alternately measures the existing actual posture and the target posture, and reduces the discrepancy between them.

Postural correction for articulated robots has been studied by many researchers. Most of these studies focused on industrial applications [1], [2], [3], [4]; in which correction within less than 1 mm was necessary to achieve accurate machining.

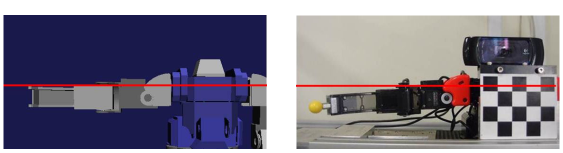

(a) Model in a simulator　　(b) Actual robot body

Fig. 1. Error in the posture of an actual robot body relative to that of the robot model

N. Hayashi, T. Tomizawa, T. Suehiro and S. Kudoh are with Graduate School of Information Systems, The University of Electro-Communications, Tokyo, Japan, e-mail: {hayashi, tomys, suehiro, kudoh }@taka.is.uec.ac.jp

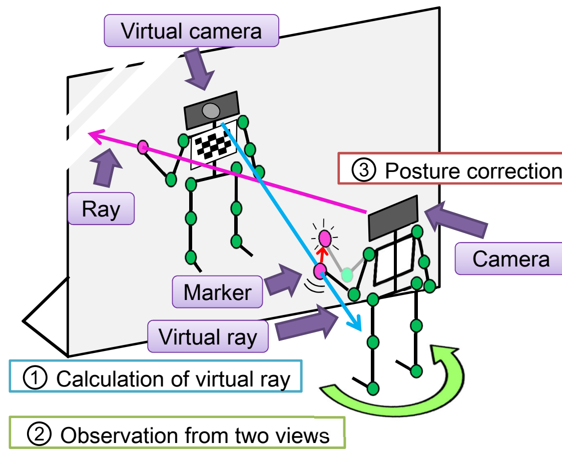

Fig. 2. Outline of the method. The robot observes its own posture in a mirror. (1) The robot calculates a virtual ray from a marker. (2) The robot observes the marker from two viewpoints and calculates the marker position by the virtual rays. (3) The robot corrects its own posture by using the marker position.

However, our method aims to correct postural errors of a small humanoid robot occurring for such mechanical reasons as backlash, transmission errors in the gears, and warping due to gravity, and so the methods proposed in the above studies are not suitable for our research. Although postural correction for humanoid robots has not been extensively investigated, a correction method for a humanoid robot that uses external cameras has been proposed [5]. In that method, a user corrects the posture of a robot on the basis of observations by external cameras. In contrast, our proposed method aims at self-correction of the robot posture.

The primary idea of our study is the use of a mirror for measuring objects. Many studies have used a mirror, primarily for calibration. On the basis of geometric constraints on a mirror, these other studies obtained the positional relationship between the camera and objects out of direct view of the camera, such as a robot [6], an IMU sensor [7], unknown coordinate frames [8], [9], and other cameras [10]. Another use of a mirror is measurement of the environment, such as 3D scene reconstruction [11], [12], [13]. A common purpose in these studies is the measuring of a coordinate frame or the position of objects not in the field of view of the camera. So, essentially, these studies considered only the geometric relationship between the camera, unknown points, and a mirror. In contrast, by observing unknown points together with a reference point whose position is known, the proposed method improves the accuracy of measurement of the mirror coordinate frame, and accordingly, improves

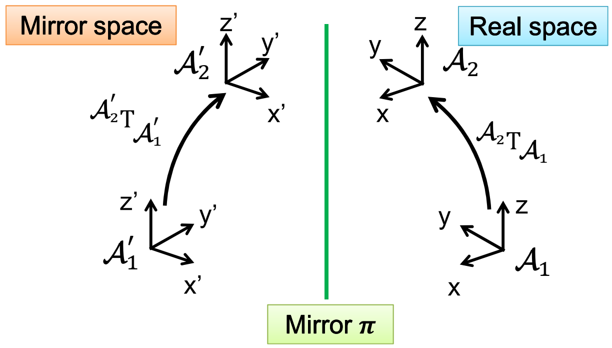

Fig. 3. Relationship between coordinates and their mirror reflections

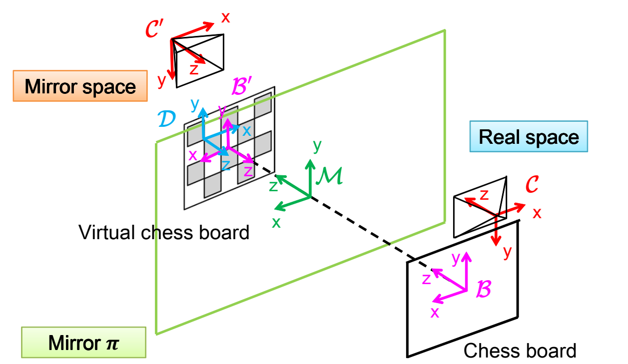

Fig. 4. Coordinate systems. $\mathcal{C}$, $\mathcal{B}$, and $\mathcal{M}$ are the coordinate systems of the camera, the chessboard, and the mirror, respectively. $\mathcal{C}'$ and $\mathcal{B}'$ are the mirror-reflected coordinate systems of $\mathcal{C}$ and $\mathcal{B}$, respectively. $\mathcal{D}$ is the base coordinate system for estimating extrinsic parameters of the camera.

the accuracy of the positional measurement of the unknown points.

The rest of this paper is organized as follows. Section II describes the proposed method of using a mirror to measure posture errors and to correct them. Section III presents the results of using an actual humanoid robot to demonstrate and evaluate the posture correction method. The conclusions are summarized in Section IV.

II. Algorithm

A. Overview

This section describes an algorithm for the measurement and correction of robot posture. The outline of the algorithm is illustrated in Fig. 2.

A humanoid robot has a camera, a chessboard, and colored markers on its body. In our implementation, the camera and the chessboard are attached on the head and the chest, respectively. The relative positions of the camera and the chessboard were calibrated beforehand. The robot stands in front of a mirror. Another camera virtually exists at the position where the real camera is reflected by the mirror (hereinafter referred to as a *virtual camera*).

The proposed algorithm consists of two steps: measurement and correction of the robot posture. First, in the measurement step, the relationship between the real camera and the virtual camera is estimated by observing the reflected chessboard through a mirror. Here, we propose a method using the geometric constraint between the mirror and objects to improve the accuracy of the estimation. Second, a ray emitted from the virtual camera to a marker is calculated (hereinafter referred to as a *virtual ray*). By observing the self-posture twice from different viewpoints, the position of the marker is calculated as the intersection of the virtual rays. In the correction step, the posture of the robot is corrected by using a Jacobian-based algorithm based on the difference between the current marker position and its proper position. The proposed algorithm gradually reduces the difference by executing the measurement and correction steps iteratively.

B. Measurement of Robot Posture

1) Coordinate Systems: We define several coordinate systems and the transformations between them. Homogeneous coordinates are used. Let $\mathcal{A}_1$ and $\mathcal{A}_2$ be two coordinate systems; then the homogeneous transformation matrix from $\mathcal{A}_1$ to $\mathcal{A}_2$ is written as

$$ {}^{\mathcal{A}_2}\mathbf{T}_{\mathcal{A}_1} = \begin{pmatrix} {}^{\mathcal{A}_2}\mathbf{R}_{\mathcal{A}_1} & {}^{\mathcal{A}_2}\mathbf{t}_{\mathcal{A}_1} \\ \mathbf{0}_3^{\mathrm{T}} & 1 \end{pmatrix}, $$

where $\mathbf{0}_3 = (0,0,0)^{\mathrm{T}}$. Let $\mathcal{A}_1'$ and $\mathcal{A}_2'$ be the mirror-reflected coordinates of $\mathcal{A}_1$ and $\mathcal{A}_2$, respectively (Fig. 3). Although $\mathcal{A}_1'$ and $\mathcal{A}_2'$ are left-handed systems, the transformation matrix between them is equal to that between $\mathcal{A}_1$ and $\mathcal{A}_2$:

$$ {}^{\mathcal{A}_2'}\mathbf{T}_{\mathcal{A}_1'} = {}^{\mathcal{A}_2}\mathbf{T}_{\mathcal{A}_1}. $$

In the proposed method, a camera and a chessboard are attached to the robot. Let $\mathcal{C}$ and $\mathcal{B}$ be the coordinate systems of the camera and the chessboard, respectively (Fig. 4). The origin of $\mathcal{B}$ is at the center of the chessboard, and the x- and y-axes lie on the chessboard plane. The relative position of the camera with respect to the chessboard is fixed, and the transformation between them, ${}^{\mathcal{C}}\mathbf{T}_{\mathcal{B}}$, is assumed to be calibrated beforehand.

Standing in front of a mirror, the robot can observe the reflection of its own chessboard in the mirror. By using a commonly used method, such as Zhang's method [14], we can estimate the transformation between the coordinate systems of the camera and the reflected chessboard, ${}^{\mathcal{C}}\mathbf{T}_{\mathcal{D}}$, where $\mathcal{D}$ denotes the coordinate system of the reflected chessboard. Since the transformation between $\mathcal{B}'$ and $\mathcal{D}$ can be determined easily, we obtain the transformation from $\mathcal{B}'$ to $\mathcal{C}$ as

$$ {}^{\mathcal{C}}\mathbf{T}_{\mathcal{B}'} = {}^{\mathcal{C}}\mathbf{T}_{\mathcal{D}}\,{}^{\mathcal{D}}\mathbf{T}_{\mathcal{B}'}. $$

Together with the known transformation ${}^{\mathcal{C}}\mathbf{T}_{\mathcal{B}}$, we obtain the transformation between the real camera and the virtual camera as

$$ {}^{\mathcal{C}}\mathbf{T}_{\mathcal{C}'} = {}^{\mathcal{C}}\mathbf{T}_{\mathcal{B}'}\,{}^{\mathcal{B}'}\mathbf{T}_{\mathcal{C}'} = {}^{\mathcal{C}}\mathbf{T}_{\mathcal{B}'}\,{}^{\mathcal{C}}\mathbf{T}_{\mathcal{B}}^{-1}. \tag{1} $$

However, as shown in the following section, the transformation ${}^{\mathcal{C}}\mathbf{T}_{\mathcal{C}'}$ calculated in this way includes many errors, primarily in the postural estimation of the reflected chessboard (i.e., the rotational component of ${}^{\mathcal{C}}\mathbf{T}_{\mathcal{D}}$), especially when the chessboard is directly in front of the camera. This error greatly affects the estimation of the robot posture. Therefore, to calculate ${}^{\mathcal{C}}\mathbf{T}_{\mathcal{C}'}$, we use another method that does not use the rotational component ${}^{\mathcal{C}}\mathbf{R}_{\mathcal{D}}$, but instead use the geometric constraints of the mirror.

Let $\mathbf{b}$ and $\mathbf{b}'$ be the origins of $\mathcal{B}$ and $\mathcal{B}'$, respectively. They are obtained as

$$ {}^{\mathcal{C}}\mathbf{b} = {}^{\mathcal{C}}\mathbf{T}_{\mathcal{B}} \begin{pmatrix} \mathbf{0}_3 \\ 1 \end{pmatrix} \quad \text{and} \quad {}^{\mathcal{C}}\mathbf{b}' = {}^{\mathcal{C}}\mathbf{T}_{\mathcal{B}'} \begin{pmatrix} \mathbf{0}_3 \\ 1 \end{pmatrix}, $$

where ${}^{\mathcal{C}}\mathbf{b}$ denotes point $\mathbf{b}$ represented with respect to $\mathcal{C}$. Since $\mathbf{b}'$ is the reflection of $\mathbf{b}$, the following relationship holds between $\mathbf{b}$, $\mathbf{b}'$, and the mirror: the mirror plane passes through the midpoint of $\mathbf{b}$ and $\mathbf{b}'$, and the normal vector of the mirror plane is parallel to $\mathbf{b}' - \mathbf{b}$. By using this relationship, the mirror plane can be determined. The mirror coordinate system $\mathcal{M}$ is defined so that the origin is at the midpoint of $\mathbf{b}$ and $\mathbf{b}'$, and the z-axis is parallel to $\mathbf{b}' - \mathbf{b}$. Since an arbitrariness remains about the x- and y-axes, we designate the x-axis to be parallel to the projection of the x-axis of $\mathcal{C}$ to the mirror plane. With this formulation, the translational and rotational components of ${}^{\mathcal{C}}\mathbf{T}_{\mathcal{M}}$ are written as

$$ {}^{\mathcal{C}}\mathbf{t}_{\mathcal{M}} = \frac{{}^{\mathcal{C}}\tilde{\mathbf{b}}' + {}^{\mathcal{C}}\tilde{\mathbf{b}}}{2} $$

$$ {}^{\mathcal{C}}\mathbf{R}_{\mathcal{M}} = \begin{pmatrix} \mathbf{m}_x & \mathbf{m}_y & \mathbf{m}_z \end{pmatrix} $$

$$ \begin{cases} \mathbf{m}_z = \dfrac{{}^{\mathcal{C}}\tilde{\mathbf{b}}' - {}^{\mathcal{C}}\tilde{\mathbf{b}}}{\|{}^{\mathcal{C}}\tilde{\mathbf{b}}' - {}^{\mathcal{C}}\tilde{\mathbf{b}}\|} \\ \mathbf{m}_x = \dfrac{\mathbf{e}_x - (\mathbf{e}_x, \mathbf{m}_z)\mathbf{m}_z}{\|\mathbf{e}_x - (\mathbf{e}_x, \mathbf{m}_z)\mathbf{m}_z\|} \\ \mathbf{m}_y = \mathbf{m}_z \times \mathbf{m}_x, \end{cases} $$

where $\mathbf{e}_x = (1, 0, 0)^{\mathrm{T}}$, and $\tilde{\mathbf{b}}$ and $\tilde{\mathbf{b}}'$ are the points in Euclidean space corresponding to points $\mathbf{b}$ and $\mathbf{b}'$ in the homogeneous space, respectively.

With respect to $\mathcal{M}$, because the coordinate systems $\mathcal{C}$ and $\mathcal{C}'$ are inverse about the z-axis, the following relationship holds:

$$ {}^{\mathcal{M}}\mathbf{T}_{\mathcal{C}'} = \mathbf{P}\,{}^{\mathcal{M}}\mathbf{T}_{\mathcal{C}} = \mathbf{P}\,{}^{\mathcal{C}}\mathbf{T}_{\mathcal{M}}^{-1}, $$

where

$$ \mathbf{P} = \begin{pmatrix} 1 & 0 & 0 & 0 \\ 0 & 1 & 0 & 0 \\ 0 & 0 & -1 & 0 \\ 0 & 0 & 0 & 1 \end{pmatrix}. $$

With the above equations, we obtain the transformation between the real camera and the virtual camera as

$$ {}^{\mathcal{C}}\mathbf{T}_{\mathcal{C}'} = {}^{\mathcal{C}}\mathbf{T}_{\mathcal{M}}\,{}^{\mathcal{M}}\mathbf{T}_{\mathcal{C}'}. \tag{2} $$

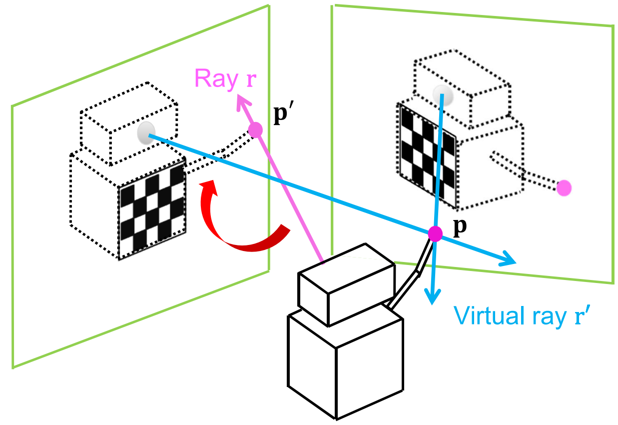

Fig. 5. Virtual rays and marker position. The virtual ray $\mathbf{r}'$ is calculated from ray $\mathbf{r}$. The marker position $\mathbf{p}$ is determined as the intersection of two virtual rays.

2) Measurement of Marker Position: In our method, the posture of the robot is estimated by measuring the position of markers attached to robot parts, such as the ends of the arms. We assume that a marker reflected in the mirror space is observed by a camera. Then, assuming that the intrinsic parameters of the camera were calibrated beforehand, we can calculate the ray from the origin of the camera to the reflected marker. The direction of the ray is represented as a homogeneous point at infinity as $\mathbf{r} = (\tilde{\mathbf{r}}^{\mathrm{T}}, 0)^{\mathrm{T}}$.

From the symmetry of a mirror, it can be said that the ray emitted from the reflected camera in the mirror space passes through the marker in the real world. Let $\mathbf{r}'$ be the direction of the virtual ray corresponding to $\mathbf{r}$. Since we define the coordinate systems $\mathcal{C}$ and $\mathcal{C}'$ symmetrically, the calculation of the virtual ray direction $\mathbf{r}'$ is totally equivalent to that of $\mathbf{r}'$. Therefore, ${}^{\mathcal{C}'}\mathbf{r}' = {}^{\mathcal{C}}\mathbf{r}$, and the virtual ray can be written as

$$ t\,{}^{\mathcal{C}'}\mathbf{r}' $$

with respect to $\mathcal{C}'$, where t $(t > 0)$ is a parameter. Transforming this by (1) or (2), we obtain the formula of the virtual ray with respect to $\mathcal{C}$ as

$$ {}^{\mathcal{C}}\mathbf{T}_{\mathcal{C}'} \left\{ \begin{pmatrix} \mathbf{0}_3 \\ 1 \end{pmatrix} + t\,{}^{\mathcal{C}'}\mathbf{r}' \right\} = \begin{pmatrix} {}^{\mathcal{C}}\mathbf{t}_{\mathcal{C}'} \\ 1 \end{pmatrix} + t \begin{pmatrix} {}^{\mathcal{C}}\mathbf{R}_{\mathcal{C}'}\,{}^{\mathcal{C}'}\tilde{\mathbf{r}} \\ 0 \end{pmatrix}. \tag{3} $$

To estimate the position of a marker, two observations from different viewpoints are required, as shown in Fig. 5. By calculating two virtual rays from the two observations using (3), the position of the marker can be obtained as the intersection of the two virtual rays. In practice, however, the two virtual rays do not always intersect due to errors. Thus, as the estimation of the marker position, we take the midpoint between the two points lying on the two rays which give the minimum distance between the two rays.

3) Correction of Robot Posture: After obtaining the position of the markers, the robot posture is corrected, if necessary, by an algorithm based on the Jacobian matrix of the marker position. We use the Jacobian matrix for the reference posture in the simulation model as an approximation of that for the actual robot posture. In practice, because the actual posture is affected by several complicated factors, such as warping and backlashes, the these two matrices are not equivalent. Hence, we iterate the correction steps until the actual posture converges to the target posture. In each step of the correction, the angles of joints $\boldsymbol{\theta}$ are updated by adding

$$\Delta\boldsymbol{\theta} = \lambda\,\mathbf{J}^{+}\Delta\mathbf{p},$$

where $\Delta\mathbf{p} = \mathbf{p}_{\mathrm{ref}} - \mathbf{p}_{\mathrm{cul}}$ ($\mathbf{p}_{\mathrm{ref}}$ and $\mathbf{p}_{\mathrm{cul}}$ are the marker positions of the designed target posture and the actual robot posture, respectively), $\mathbf{J}^{+}$ is the pseudo-inverse of the Jacobian matrix, and λ is a gain. Algorithm 1 summarizes the above description.

The reason for using gain λ is as follows. If a joint angle overshoots an appropriate angle due to a correction step, it can harm the convergence of the iteration because the actuators often have different rotational directions. Therefore, we introduce a small gain λ so that the marker position approaches the target position gradually.

Algorithm 1 Posture_Correction ($\boldsymbol{\theta}_{\mathrm{ref}}$, $\mathbf{p}_{\mathrm{ref}}$, λ)

```
θ ← θ_ref
J⁺ ← J(θ_ref)⁺
loop
   Observing p_cul
   Δp ← p_ref − p_cul
   if ‖Δp‖ < ε then
      return
   end if
   θ ← θ + λ J⁺ Δp
end loop
```

III. Experiment

A. Experimental Setup

The humanoid robot used for the experiments consists of the following equipment:

Robot: G-ROBOT (HPI), Height: 255 mm
Chessboard: 14 mm × 14 mm for each square
Finger markers: Sphere diameter: 11.6 mm
Head camera: Webcam C910 (Logitech)
Resolution of an image: Resolution: 800 × 600 pixels
Mirror: Glass mirror, thickness: 3 mm

The relationship between the camera and the chessboard is calibrated by using another camera and chessboard. The new chessboard is set in the field of view of the robot's camera. The new camera is set in a place where it can observe both chessboards. The relationship between the robot's camera and the robot's chessboard is derived from the relationships of these cameras and these chessboards.

The position of the markers in the images are detected by color extraction and labeling. It is assumed that the region of a marker is always larger than any other regions that have the same color as the marker.

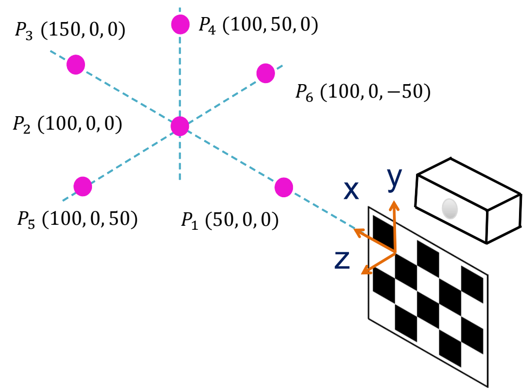

Fig. 6. Marker position used in the experiments

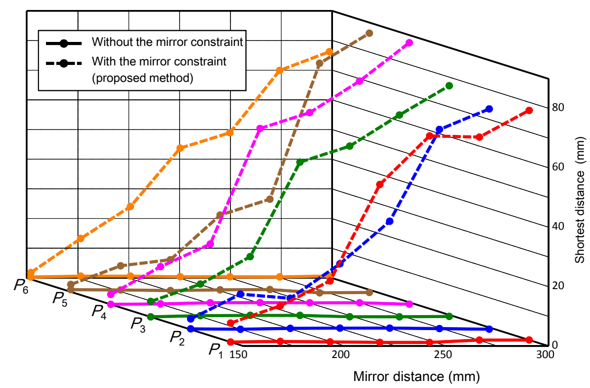

Fig. 7. Shortest distance between the virtual rays and the corresponding markers against the distance between the robot and the mirror. Dashed lines show the results without the mirror constraint by Eq(1) . Solid lines show the results with the mirror constraint by Eq(2) (the proposed method).

B. Measurement of Robot Posture

1) Evaluation of Accuracy of Virtual Ray: In this experiment, we evaluate the calculation of a virtual ray. As shown in Fig. 6, we placed markers at six places. After calculating virtual rays for the six markers, we measured the shortest distance between the virtual rays and the corresponding markers 100 times and calculated the average. In calculating the virtual rays, we took two approaches: with the mirror constraint (the approach based on (2)) and without it (the approach based on (1)), and compared the results.

First, we examined the influence of the distance between the robot and the mirror. The chessboard was placed directly in front of the mirror at distances varying from 150 mm to 300 mm. Figure 7 shows the averages of the shortest distance. To see the details, we replotted the result for marker position P_1 in Fig. 8 as an example. When not using the mirror constraint, the error increased as the distance from the mirror increased. In contrast, when using the mirror constraint (the proposed method), the errors were low, which means that the distance did not have a great affect on the error.

Second, we examined the influence of the angle between the robot and the mirror. The chessboard was placed 150 mm from the mirror and rotated between $-15°$ and $25°$. We measured a marker at known position P_2. Figure 9 shows the average of the shortest distance. When not using the

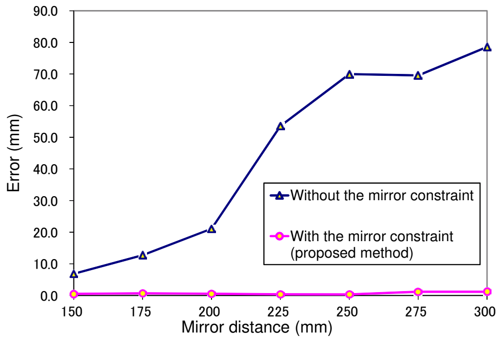

Fig. 8. Shortest distance between the virtual ray and the marker (the case of P_1)

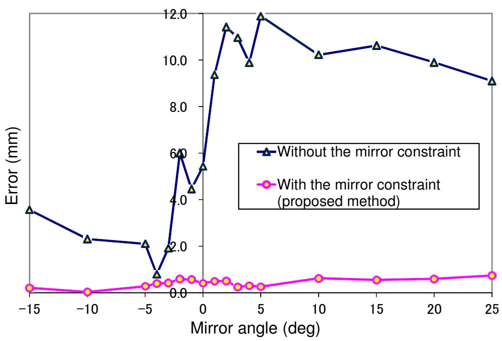

Fig. 9. Shortest distance between the virtual ray and the marker against the angle between the robot and the mirror

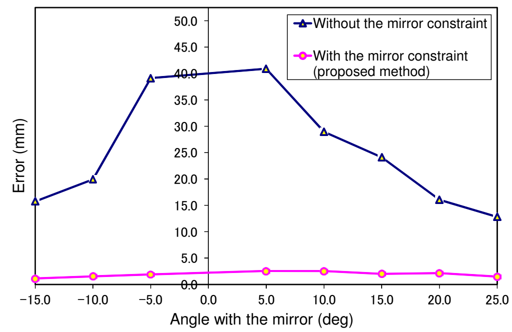

Fig. 10. Error in measurement of the marker position against the angle between the robot and the mirror

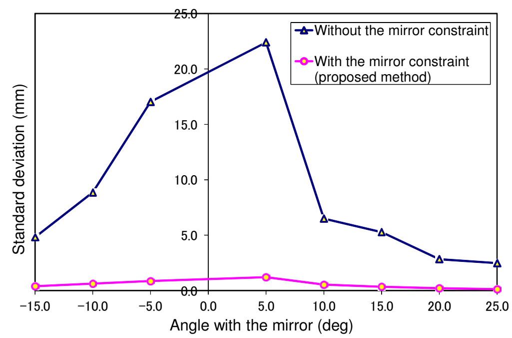

Fig. 11. Standard deviation of measurement of the marker position against the angle between the robot and the mirror

mirror constraint, the error notably increased around 0°. In comparison, the error was low for all angles when using the mirror constraint. Consequently, using the geometric constraint involving the mirror also increases the measurement accuracy of the virtual ray.

2) Evaluation of Accuracy of Marker Position: Next, we evaluated the accuracy of measuring the position of a marker. Our method measures the position of a marker by using two observation points. We set a marker at known position P_2 in Fig. 6 and the chessboard at a distance 150 mm from the mirror. We took ten measurements of the position of the marker with and without the mirror constraint. Figures 10 and 11 show the mean and the standard deviation of the error of the estimated position, respectively. We can see from these figures that the proposed method with the mirror constraint is not affected by the angle of observation and significantly improves the accuracy and precision of the measurement.

C. Correction of Robot Posture

1) Evaluation of Accuracy of Posture Correction: In this experiment, we evaluated the correction method. The upper body of the robot was fixed on a measurement stand, and the distance between the chessboard and the mirror was 150 mm. A marker was attached to the tip of the right hand. Three joints are between the marker and the chessboard, as shown in Fig. 12. When measuring the position of the marker, we captured two images in the mirror from the viewpoints in which the angles between the chessboard and the mirror were 0° and 15°. The joint angles of the target posture were set

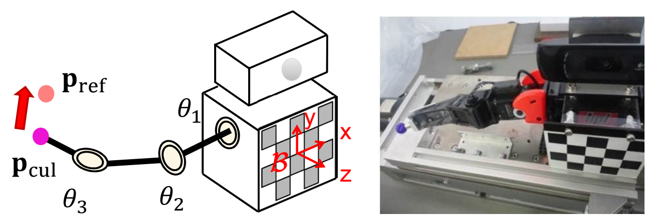

(a) The model of joints (b) The actual robot

Fig. 12. Setup for the experiment of posture correction

TABLE I
ERROR IN THE POSITION OF THE HAND MARKER

	x	y	z	d
Error (mm)	1.7	7.6	−5.1	9.3

for $(\theta_1, \theta_2, \theta_3)^{\mathrm{T}} = (-15°, 85°, 15°)^{\mathrm{T}} \equiv \boldsymbol{\theta}_{\mathrm{ref}}$.

At the beginning, the joint angles of the robot were set for $\boldsymbol{\theta}_{\mathrm{ref}}$. The discrepancy at this moment in the position of the marker between the initial posture of the actual body and the model is shown in TABLE I. Here, the difference between the two points are represented in three axial directions in the chessboard frame (x, y, z) and in the Euclidean distance (d).

We conducted postural corrections for five different values of the gain: $\lambda = 0.2, 0.4, 0.6, 0.8$, and 1.0. For each postural correction, we executed four iterations. For each iteration step, we measured the distance between the current marker position and the target position, d. We conducted this experiment five times. Figure 13 shows the distance d, where each value of d is the mean value of the five measurements.

The method reduced the positional error in the correction

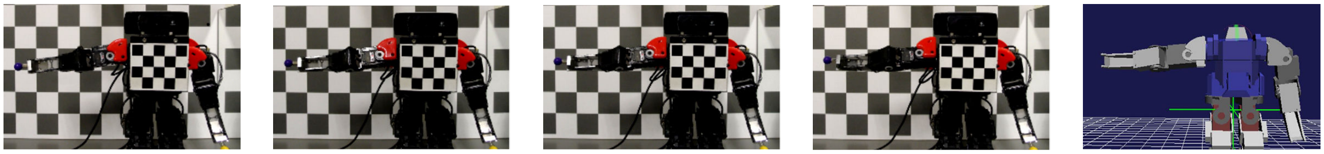

(a) Initial posture (b) 1st correction (c) 2nd correction (d) 3rd correction (e) Target posture

Fig. 14. Posture correction using the leg of the humanoid robot for changing the viewpoints.

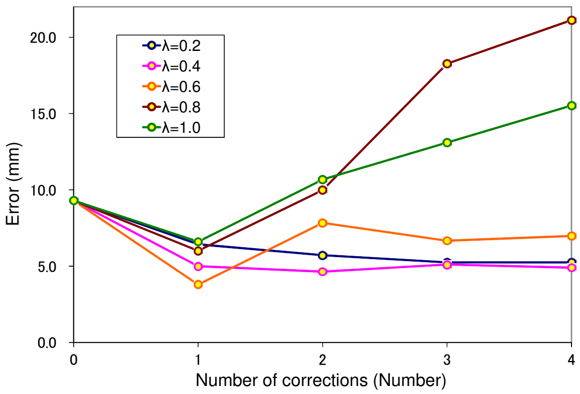

Fig. 13. Error convergence by iterations depending on λ

for all λ values. When the gain was small, such as $\lambda = 0.2$, the positional error converged. As described above, this was because the small value of λ prevented overshooting of the joint angles. Finally, the method could reduce the positional error of the hand to within 5 mm when λ was set to an appropriate value.

2) Posture Correction Using Leg of Humanoid: In the previous experiments, we fixed the upper body of the humanoid on a measurement stand in order to measure the error accurately. In this experiment, we rotated the robot on its own legs. The target posture was $\theta_1 = -15°$, $\theta_2 = 85°$, and $\theta_3 = 15°$. We set the gain to $\lambda = 0.2$. Figure 14 shows the position of the robot at each correction step, and we can see that the warped posture was successfully corrected by the proposed method.

IV. Conclusions

In this paper, we proposed a new method in which humanoid robots use their image in a mirror to self-correct their postural errors. This method requires only a mirror in front of a robot. No additional time-consuming setup, such as calibration of external cameras, is necessary. We used the geometric relationship of a mirror, a camera, and reference points when the relative position of the camera and the reference points is known. On the basis of this relation, our proposed method can improve the accuracy of the posture measurement. Also, we proposed a method for correcting the posture of a humanoid robot. By alternately measuring the posture and the desired correction, we can reduce the discrepancies between the actual posture and the target posture.

Acknowledgement

This work was supported by JSPS KAKENHI Grant Number 23240026.

References

[1] Daney D., Papegay Y., Madeline B., "Choosing Measurement Poses for Robot Calibration with the Local Convergence Method and Tabu Search", International Journal of Robotics Research Archive 24(6), pp. 501-518, June 2005.

[2] Fujioka J., Aoyagi S., Ishii K., Seki H., Kamiya T. "Study on Robot Calibration Using a Laser Tracking System (2nd Report): Discussion on How to Select Parameters, Number of Measurement and Pose of Measurement in Multiple Positioning Method", Journal of the Japan Society for Precision Engineering 67(4), pp. 676-682, 2001.

[3] Okada T., Mori S., "A Method to Correct Structural Errors of Articulated Robots", Transactions of the Japan Society of Mechanical Engineers, Series C, 51(462), pp. 324-331, 1985-02-25.

[4] Touyama S., "Error Analysis of Robot Manipulator (Special Issue on Three-coordinate Motion Mechanism)", Journal of the Japan Society for Precision Engineering, 52(8), pp. 1309-1312, 1986-08-05.

[5] Ishikawa T., Hasegawa S., "Virtual stroboscope for robot motion design", Special Interest Group on Computer GRAPHics(ACM SIGGRAPH), 2009.

[6] Hesch J.A., Mourikis A.I., Roumeliotis S.I., "Mirror-based extrinsic camera calibration", Algorithmic Foundation of Robotics VIII, pp. 285-299, 2009.

[7] Panahandeh G., Jansson M., "IMU-camera self-calibration using planar mirror reflection", Indoor Positioning and Indoor Navigation (IPIN), 2011.

[8] Takahashi K., Nobuhara S., Matsuyama T., "A New Mirror-based Extrinsic Camera Calibration Using an Orthogonality Constraint", Conference on Computer Vision and Pattern Recognition(CVPR), 2012.

[9] Rodrigues R., Barreto J., Nunes U., "Camera pose estimation using images of planar mirror reflections", European conference on Computer vision (ECCV), Part IV, LNCS 6314, pp. 382-395, 2010.

[10] Kumar R., Ilie A., Frahm J.M., Pollefeys M., "Simple calibration of non-overlapping cameras with a mirror", Conference on Computer Vision and Pattern Recognition (CVPR), 2008.

[11] Mariottini G.L., Scheggi S., Morbidi F., Prattichizzo D., "Planar Mirrors for Image-based Robot Localization and 3-D Reconstruction", Mechatronics, 22, pp. 398-409, 2012.

[12] Jang K.H., Lee D.H., Jung S.K., "A moving planar mirror based approach for cultural reconstruction: Research Articles", Computer Animation and Virtual Worlds, 15, pp. 415-423, 2004.

[13] Gluckman J., Nayar S.K. , "Planar Catadioptric Stereo: Geometry and Calibration", Conference on Computer Vision and Pattern Recognition (CVPR), Vol.1, pp.22-28, Jun, 1999.

[14] Zhang Z., "A flexible new technique for camera calibration", Transactions on Pattern Analysis and Machine Intelligence, 22(11), pp. 1330-1334, 2000.